IOPscience iopscience.iop.org

Home Search Collections Journals About Contact us My IOPscience

Growth and structural properties of silicene at multilayer coverage

This content has been downloaded from IOPscience. Please scroll down to see the full text.

2014 J. Phys.: Condens. Matter 26 185003

(http://iopscience.iop.org/0953-8984/26/18/185003)

View the table of contents for this issue, or go to the journal homepage for more

Download details:

IP Address: 129.120.87.225
This content was downloaded on 07/02/2017 at 17:19

Please note that terms and conditions apply.

You may also be interested in:

Presence of gapped silicene-derived band in the prototypical (3times3) silicene phase on silver (111) surfaces
J Avila, P De Padova, S Cho et al.

The quasiparticle band dispersion in epitaxial multilayer silicene
Paola De Padova, Jose Avila, Andrea Resta et al.

Two dimensional silicon: the advent of silicene
Carlo Grazianetti, Eugenio Cinquanta and Alessandro Molle

Growth of silicene layers on Ag(111): unexpected effect of the substrate temperature
H Jamgotchian, Y Colignon, N Hamzaoui et al.

Bottom-up fabrication of graphene nanostructures on Ru(1010)
Junjie Song, Han-jie Zhang, Yiliang Cai et al.

A comprehensive study of the (23×23)R30° structure of silicene on Ag(111)
H Jamgotchian, B Ealet, Y Colignon et al.

Various atomic structures of monolayer silicene fabricated on Ag(111)
Zhi-Long Liu, Mei-Xiao Wang, Jin-Peng Xu et al.

IOP Publishing Journal of Physics: Condensed Matter
J. Phys.: Condens. Matter **26** (2014) 185003 (4pp) doi:10.1088/0953-8984/26/18/185003

Growth and structural properties of silicene at multilayer coverage

E Salomon, R El Ajjouri, G Le Lay and T Angot

Aix-Marseille Université, CNRS, PIIM UMR 7345, 13397, Marseille, France

E-mail: eric.salomon@univ-amu.fr

Received 22 November 2013, revised 21 February 2014
Accepted for publication 21 February 2014
Published 14 April 2014

Abstract

At monolayer coverage, silicene on Ag(1 1 1) may present different structural phases depending on the growth conditions. At multilayer coverage, only one structural phase has been reported: the $(\sqrt{3}\times\sqrt{3})R30°$ phase. However, no link between the structural arrangement of the monolayer and that of the multilayer has been addressed. In this paper, reporting experimental work based on low-energy electron diffraction and scanning tunneling microscopy, we focus on the structural aspects of a multilayer film of silicene. We demonstrate that it exhibits one structural arrangement, namely the $(\sqrt{3}\times\sqrt{3})R30°$ form, but with different domain orientations resulting from the structural properties of the initial wetting monolayer.

Keywords: silicene, multilayer, growth, scanning tunneling microscopy

(Some figures may appear in colour only in the online journal)

1. Introduction

Since the discovery of the exotic and outstanding properties of graphene, two-dimensional (2D) systems have seen a tremendous gain in interest. Hence, a strong activity to develop graphene-like 2D materials has grown up during the past few years [1]. Among these materials, silicene, the silicon analogue of graphene, is one of the most attractive, because of its possible compatibility with the existing technologies in microelectronics. The possibility of obtaining the silicon equivalent of graphene was first mentioned in a theoretical study led by Takeda and Shiraishi in 1994 [2]. The term silicene was further introduced by Guzman-Verri *et al* in 2007 to describe graphene-like silicon based 2D materials. From that time, several theoretical calculations related to free-standing silicene have demonstrated that it presents physical properties similar to those of graphene, such as a Dirac fermion electronic dispersion [2–8]. Moreover, due to its stronger spin–orbit coupling, silicene appears as a good candidate for showing 2D topological insulator behavior as well as the quantum spin Hall effect [6, 9–11].

Although it has not yet been proven that one can synthesize pure free-standing silicene, in 2012 compelling experimental and theoretical evidence of silicene sheets exhibiting graphene-like physical properties was presented [12]. By adsorbing silicon atoms on a Ag(1 1 1) surface, the authors showed that it is possible to grow, at monolayer coverage, a buckled honeycomb lattice of silicon atoms presenting a Dirac fermion-like electronic dispersion [12, 13]. The structural arrangement of the silicon atoms was identified and corresponds to a (3×3) reconstruction with respect to the silicene unit cell, i.e. a (4×4) form with respect to the Ag(1 1 1) unit cell [12, 14–18]. However, angularly resolved photoemission spectroscopy (ARPES) measurements show that there is a band gap that should be approximately 0.6 eV between the π and the π^* bands. The origin of this gap is the buckled structure of silicene-(3×3) [19]. Since then, numerous experimental papers describing the structural and/or electronic properties of silicene on various metallic surfaces have been published, demonstrating the strong interest of the scientific community [14–18, 20–27]. Most of these works treat the physical properties of the first layer of silicene. It appears that for silicon deposited onto Ag(1 1 1), different phases appear depending on the substrate temperature and the coverage [15, 18, 22, 23]. This results from a subtle balance between aspects of different processes: the evaporation rate and the kinetics of diffusion in the bulk (solubility) or along the Ag surface. While the (3×3) phase has been clearly identified as the most stable epitaxial silicene phase, another reconstruction forming a $(\sqrt{7}\times\sqrt{7})R19.1°$ structure with respect to the silicene unit cell, i.e. a $(\sqrt{13}\times\sqrt{13})R13.4°$ form with

 © 2014 IOP Publishing Ltd Printed in the UK

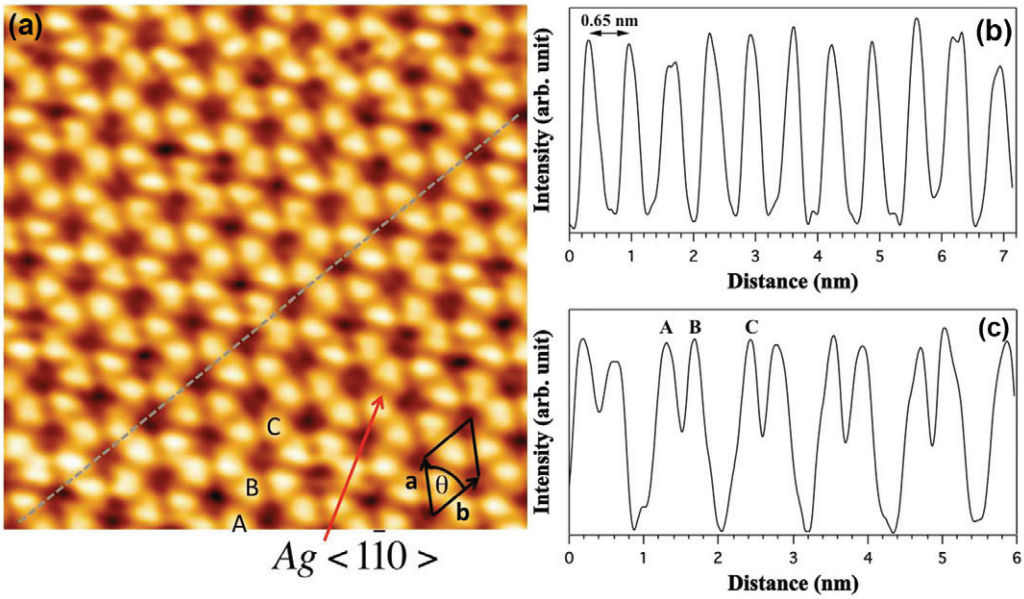

Figure 1. (*a*) 5.7 nm × 5.7 nm high-resolution STM image of the silicene-$(\sqrt{3}\times\sqrt{3})R30°$ phase. Tunneling parameters: I_t = 0.16 nA, bias = −560 mV (occupied states). The black rhombus represents the silicene unit cell (see the text for more details). (*b*) Line profile along the dashed gray line indicated in (*a*). (*c*) Line profile along the Ag [1 $\bar{1}$ 0] direction.

respect to the Ag(1 1 1) unit cell, could be another possible candidate [18].

At multilayer coverage, the situation is different. Indeed, for coverages above one monolayer the silicene seems to exhibit only one structural phase corresponding to a $(\sqrt{3}\times\sqrt{3})R30°$ reconstruction with a lattice parameter of 6.67 Å [15, 16, 18, 28, 29]. Even though the existence and the physical origin of Dirac electrons in silicene films grown on Ag(1 1 1) are still under debate, and subject to some controversy, very recent ARPES measurements recorded on the $(\sqrt{3}\times\sqrt{3})R30°$ phase exhibit a Dirac fermion electronic dispersion with no band gap, like that in graphene [8, 13, 17, 20, 28–31]. Moreover, the Dirac point lies 0.25 eV below the Fermi level, which means that as in the case of graphene grown on SiC, the silicene- $(\sqrt{3}\times\sqrt{3})R30°$ appears to be intrinsically n-type doped. Nevertheless, despite the work that has been done so far, the growth process of the multilayer film and a detailed description of its structural arrangement have not been addressed and remain unclear.

Hence, in this paper we investigate the structural properties of a multilayer film of silicene grown on Ag(1 1 1) by means of scanning tunneling microscopy (STM) and low-energy electron diffraction (LEED). We show that the structural properties of the first silicene layer strongly influence those of the multilayer. More particularly, we demonstrate that several rotated domains of the silicene-$(\sqrt{3}\times\sqrt{3})R30°$ phase coexist. We established that these different orientations correspond to growth of both the (3 × 3) and the $(\sqrt{7}\times\sqrt{7})R19.1°$ phases of the first wetting layer of silicene.

2. The experimental setup

Experiments were performed in a series of interconnected ultrahigh-vacuum chambers equipped for standard surface preparation techniques, LEED, STM, and high-resolution electron energy loss spectroscopy (HREELS) analysis. The silver single-crystal surface has been prepared by several cycles of sputtering with argon ions and annealing up to 750 K for 30 min. The cleanliness and order of the substrate have been further checked by means of HREELS, LEED and STM. The silicon was thermally evaporated from a piece of silicon wafer heated up to 1 300 K by direct current with a rate of about 0.05 ML min^{-1}. The silicene multilayer was grown in a single evaporation of 120 min, keeping the silver substrate at 510 K. All measurements have been realized under ultrahigh-vacuum conditions at room temperature (RT). The LEED optics used were a SpectaLeed Omicron system. STM images were acquired by using a commercial Omicron VT-STM. Home-made STM tips were fabricated from electrochemically etched tungsten wires in 2 M NaOH solution. STM images were recorded in constant-current mode and processed using the WSxM software [32]. Linear electronic drift correction was systematically used to compensate for possible thermal and mechanical drift of the probe.

3. Results and discussion

Figure 1(*a*) exhibits a high-resolution STM micrograph of the multilayer film. In the image, one can clearly observe dark holes surrounded by six bright protrusions forming a honeycomb arrangement. The line profile displayed in figure 1(*b*) was recorded along the light dashed–dotted line indicated on the STM image. It shows that the periodicity of the dark holes is 6.5 ± 0.2 Å. Its basis vectors are rotated by 30 ± 1° from those of Ag(1 1 1) and the unit cell parameters are the following: $a = b = 6.5 \pm 0.2$ Å; $\theta = 60 \pm 1°$. As expected for a multilayer film of silicene, these values actually match those already reported for the $(\sqrt{3}\times\sqrt{3})R30°$ reconstruction [13, 15, 16, 18, 20]. Here, the notation $(\sqrt{3}\times\sqrt{3})R30°$ is with respect to the

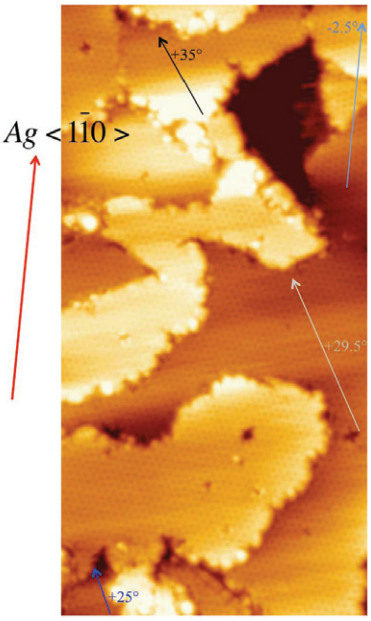

Figure 2. 56 nm × 28 nm STM micrograph of silicene-$(\sqrt{3}\times\sqrt{3})R30°$. Tunneling parameters: $I_t = 0.27$ nA, bias = −1.12 mV (occupied states). The light blue, dark blue, gray and black arrows represent the orientations of the different domains, and are respectively rotated by −2.5°, 25.0°, 29.5° and 35.0° ±1.5° from the Ag [1 $\bar{1}$ 0] direction.

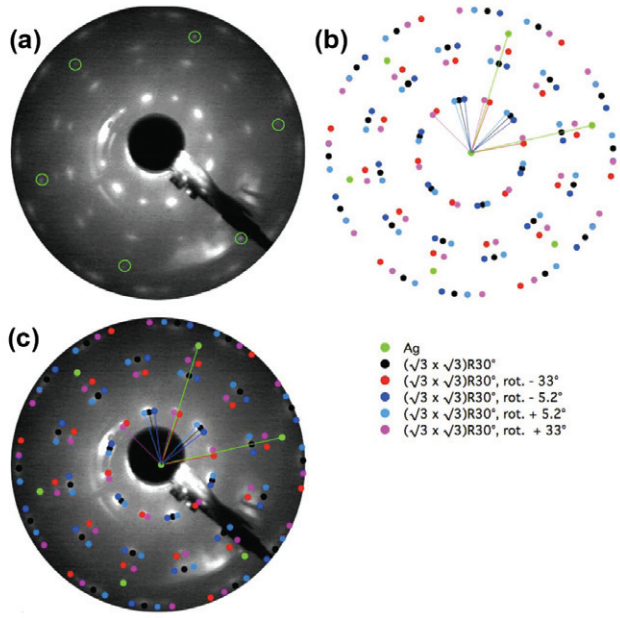

Figure 3. (*a*) LEED pattern of the multilayer silicene-$(\sqrt{3}\times\sqrt{3})R30°$ recorded at 75 eV. The green circle represents the spots of the Ag(1 1 1) substrate. (*b*) LEED pattern simulation of a $(\sqrt{3}\times\sqrt{3})R30°$ reconstruction presenting the following five different orientations: −3.0°; −24.8°; 30°; 35.2°; 63.0°, with respect to the Ag [1 $\bar{1}$ 0] direction. (*c*) Superposition of (*a*) and (*b*).

silicene unit cell at monolayer coverage. It corresponds to $(4/\sqrt{3} \times 4/\sqrt{3})R30°$ with respect to the Ag(1 1 1) unit cell [15]. Finally, figure 1(*c*) corresponds to a line profile recorded along the Ag [1$\bar{1}$0] direction. From this profile, one can establish that the distance between two nearest-neighbor bright protrusions ($\overline{AB}$) is 3.8 ± 0.2 Å. The distance between two opposite vertices of a hexagon ($\overline{BC}$) is 7.5 ± 0.2 Å, i.e. twice $\overline{AB}$. Finally the $\overline{AC}$ distance is 11.5 ± 0.2 Å, i.e. three times $\overline{AB}$. These values are actually in good agreement with previous results and models of the honeycomb-like $(\sqrt{3}\times\sqrt{3})R30°$ superstructure of silicene [13, 16, 20, 33].

Figure 2 displays a larger scale image of the multilayer film. A thorough analysis demonstrates that several domains of the $(\sqrt{3} \times \sqrt{3})R30°$ phase, with different orientations, are coexisting. In the micrograph, one can actually identify four distinct orientations as indicated by the light blue, dark blue, gray and black arrows. These domains are respectively rotated by −2.5°, 25.0°, 29.5° and 35.0° ±1.5° from the Ag [1$\bar{1}$0] direction (red arrow).

To further understand these diverse orientations of the multilayer silicene, let us recall that close to monolayer coverage, different phases, with various orientations, can coexist [15, 18, 22]. In a recent work, Resta *et al* have shown that the first layer of silicene mainly adopts a (3 × 3) reconstruction with respect to the silicene unit cell. But they also demonstrate that this phase may coexist with four different rotational domains, rotated by −33.0°, −5.2°, +5.2° and +33.0° from the Ag [1$\bar{1}$0] direction, of a different superstructure corresponding to a $(\sqrt{7}\times\sqrt{7})R19.1°$ phase of silicene. In this latter phase the Si–Si bonds would be expanded by 2% as compared to the (3 × 3) phase [18]. Therefore, we consider that in the present work, the growth occurred as follows. First, during the evaporation process, we produced a first layer presenting similar structural properties to the one described by Resta *et al*, i.e. in which the (3 × 3) phase and the four equivalent rotational domains of the $(\sqrt{7}\times\sqrt{7})R19.1°$ were coexisting. Then, sustaining the evaporation, we started growing the multilayer on top of this initial layer, which results in the formation of a $(\sqrt{3}\times\sqrt{3})R30°$ reconstruction exhibiting five different rotational domains. According to the orientations of the domain of the first layer, five domains of the $(\sqrt{3}\times\sqrt{3})R30°$ phase can be expected, respectively oriented at −3.0°, 24.8°, 30°, 35.2° and 63.0° from the Ag [1$\bar{1}$0] direction. These values are actually in fairly good agreement with those measured on the STM image presented in figure 2, although, unfortunately, we were not able to observe the fifth domain, at 63°. This demonstrates that upon growing silicene at multilayer coverage, the first-layer domains constitute different wetting layers whose orientations directly induce the structural and final arrangement of the multilayer film.

To further support this, we performed diffraction experiments on the silicene- $(\sqrt{3}\times\sqrt{3})R30°$. Figure 3(*a*) displays the LEED pattern of the multilayer film.

One can clearly distinguish, besides those from the silver substrate (green circle), many diffraction spots due to the film. These diffraction spots are not as sharp as those of the Ag(1 1 1), for two main reasons. The first one is the size of the $(\sqrt{3}\times\sqrt{3})R30°$ domains—which is much smaller than that of the terraces of the Ag(1 1 1), due to the presence of differently oriented domains. Then, as a matter of fact, because of these coexisting domains, each broad spot observed experimentally actually results from the superposition of several patterns

too close to be resolved experimentally. This point is further confirmed by performing a simulation of the LEED pattern expected for a surface exhibiting the five expected different rotations of the $(\sqrt{3}\times\sqrt{3})R30°$ form, as described above. The result is displayed in figure 3(*b*). For the sake of comparison, we also added the diffraction spots of the Ag(1 1 1) substrate. In the simulation of the pattern, one can clearly observe that the diffraction spots are spatially distributed within a few groups made up of several individual spots. Each of these groups lies within a broad diffraction spot, observed experimentally. This point is more clearly illustrated in figure 3(*c*), which corresponds to the superposition of the experimental LEED pattern and the simulation. In the figure, both images have been scaled using the diffraction spots of the Ag(1 1 1). The good agreement between theoretical and experimental data shows that our LEED pattern is well explained by a $(\sqrt{3}\times\sqrt{3})R30°$ superstructure with five different domains rotated at −3.0°, −24.8°, 30°, 35.2° and 63.0° from the Ag $[1\bar{1}0]$ direction, supporting the STM observations described above.

Combining STM and LEED measurements, we have confirmed that at multilayer coverage the silicene adopts a unique $(\sqrt{3}\times\sqrt{3})R30°$ reconstruction. We have further established that several rotational domains of this superstructure may coexist and that their orientations are determined by the structural arrangement of the first silicene layer. In this report, we emphasized that the orientations of the different rotational domains observed at multilayer coverage correspond to those observed in the monolayer regime. Therefore, it is clear that during the process of growth of multilayer silicene, the structural properties of the wetting monolayer directly determine those of the multilayer film.

Acknowledgments

This work was supported by the '2D-NANOLATTICES' project of the Future and Emerging Technologies (FET) program within the 7th framework program for research of the European Commission, under FET Grant No. 270749.

References

[1] Xu M, Liang T, Shi M and Chen H 2013 *Chem. Rev.* **113** 3766
[2] Takeda K and Shiraishi K 1994 *Phys. Rev.* B **50** 14916
[3] Guzman G G and Lew L C 2007 *Phys. Rev.* B **76** 075131
[4] Lebegue S and Eriksson O 2009 *Phys. Rev.* B **79** 115409
[5] Cahangirov S, Topsakal M, Akturk E S, Sahin H and Ciraci S 2009 *Phys. Rev. Lett.* **102** 236804
[6] Ezawa M 2012 *Phys. Rev. Lett.* **109** 055502
[7] Gao J and Zhao J 2012 *Sci. Rep.* **2** 861
[8] Huang S, Kang W and Yang L 2013 *Appl. Phys. Lett.* **102** 133106
[9] Ezawa M 2013 *Eur. Phys. J.* B **86** 139
[10] Liu C C, Feng W and Yao Y G 2011 *Phys. Rev. Lett.* **107** 076802
[11] Liu C C, Jiang H and Yao Y G 2011 *Phys. Rev.* B **84** 195430
[12] Vogt P, De P, Quaresima C, Avila J, Frantzeskakis E, Asensio M C, Resta A, Ealet B and Le G 2012 *Phys. Rev. Lett.* **108** 155501
[13] Chen L, Liu C C, Feng B, He X, Cheng P, Ding Z, Meng S, Yao Y G and Wu K H 2012 *Phys. Rev. Lett.* **109** 056804
[14] Lin L, Arafune R, Kawahara K, Tsukahara N, Minamitani E, Kim Y, Takagi N and Kawai M 2012 *Appl. Phys. Express* **5** 045802
[15] Arafune R, Lin L, Kawahara K, Tsukahara N, Minamitani E, Kim Y, Takagi N and Kawai M 2012 *Surf. Sci.* **608** 297
[16] Feng B, Ding Z, Meng S, Yao Y, He X, Cheng P, Chen L and Wu K 2012 *Nano Lett.* **12** 3507
[17] Lin L, Arafune R, Kawahara K, Kanno M, Tsukahara N, Minamitani E, Kim Y, Kawai M and Takagi N 2013 *Phys. Rev. Lett.* **110** 076801
[18] Resta A, Leoni T, Barth C, Ranguis A, Becker C, Bruhn T, Vogt P and Le G 2013 *Sci. Rep.* **3** 2399
[19] Avila J, De P, Cho S, Colambo I, Lorcy S, Quaresima C, Vogt P, Resta A, Le G and Asensio M C 2013 *J. Phys.: Condens. Matter* **25** 262001
[20] Chen L, Li H, Feng B, Ding Z, Qui J, Cheng P, Wu K and Meng S 2013 *Phys. Rev. Lett.* **110** 085504
[21] Chen L, Feng B and Wu K 2013 *Appl. Phys. Lett.* **102** 081602
[22] Chiappe D, Grazianetti C, Tallarida G, Fanciulli M and Molle A 2012 *Adv. Mater.* **24** 5988
[23] Jamgotchian H, Colignon Y, Hamzaoui N, Ealet B, Hoarau J Y, Aufray B and Biberian J P 2012 *J. Phys.: Condens. Matter* **24** 172001
[24] Le G, De P, Resta A, Bruhn T and Vogt P 2012 *J. Phys. D: Appl. Phys.* **45** 392001
[25] Meng L et al 2013 *Nano Lett.* **13** 685
[26] Fleurence A, Friedlein R, Ozaki T, Kawai H, Wang Y and Yamada Y 2012 *Phys. Rev. Lett.* **108** 245501
[27] Majzik Z, Tchalala M R, Svec M, Hapala P, Enriquez H, Kara A, Mayne A J, Dujardin G, Jelinek P and Oughaddou H 2013 *J. Phys.: Condens. Matter* **25** 225301
[28] De P et al 2013 *Appl. Phys. Lett.* **102** 163106
[29] De P et al 2013 *J. Phys.: Condens. Matter* **25** 382202
[30] Guo X, Furuya S, Iwata J and Oshiyama A 2013 *J. Phys. Soc. Japan* **82** 063714
[31] Guo X, Furuya S, Iwata J and Oshiyama A 2013 *Phys. Rev.* B **87** 235435
[32] Horcas I, Fernandez R, Gomez J M, Colchero J, Gomez J and M A 2007 *Rev. Sci. Instrum.* **78** 013705
[33] Kaltsas D and Tsetseris L 2013 *Phys. Chem. Chem. Phys.* **15** 9710